https://doi.org/10.1016/j.microc.2019.104469

CITATION

Nicole de Manincor, Giacomo Marchioro, Enrico Fiorin, Marco Raffaelli, Ornella Salvadori, Claudia Daffara, "Integration of multispectral visible-infrared imaging and pointwise X-ray fluorescence data for the analysis of a large canvas painting by Carpaccio", Microchemical Journal, Volume 153, 2020, 104469, https://doi.org/10.1016/j.microc.2019.104469.

Integration of multispectral visible-infrared imaging and pointwise X-ray fluorescence data for the analysis of a large canvas painting by Carpaccio

Nicole de Manincor[a], Giacomo Marchioro[b], Enrico Fiorin[c], Marco Raffaelli[d], Ornella Salvadori[c], Claudia Daffara[b]*

[a] Dept. of Cultures and Civilizations, Viale dell'Università 4, 37129 Verona, Italy

[b] Dept. of Computer Science, University of Verona, Strada le Grazie 15, 37134 Verona, Italy

[c] Gallerie dell'Accademia di Venezia, Scientific Laboratory of Misericordia, Cannaregio 3553, 30121 Venice, Italy

[d] CNR - National Institute of Optics, Largo Enrico Fermi 6, 50125 Florence, Italy

*Corresponding author: claudia.daffara@univr.it

Abstract

In this work, we studied the canvas "The meeting of the pilgrims with the Pope" by Vittore Carpaccio fusing in a single data structure the pointwise XRF analysis with the Vis-IR multispectral data acquired on the painting. We proposed a workflow for analyzing and interpreting the data using Principal Component Analysis. The effectiveness of this approach is evaluated against the analysis of the data analyzed as separated contributions. The proposed procedure is demonstrated on the red pigments, which are predominant in this painting and in Carpaccio's production in general, highlighting information regarding the original artist's technique and regarding restored areas.

KEYWORDS

Artwork nondestructive diagnostics

Multispectral infrared imaging

False colour imaging

X-ray fluorescence (XRF)

Principal Component Analysis (PCA)

1. Introduction

Nowadays, noninvasive analysis of artworks is being performed thanks to a wide range of available imaging-based and spectrometry-based techniques that exploit optical and non-optical ranges to probe the artifact's materials [1-3].

Among the imaging methods, multispectral imaging in the IR range based on the acquisition of narrow-band reflectance images from 0.8 up to 2.5 μm (NIR) is a powerful and versatile tool for the diagnostics of ancient paintings, as the multispectral cube can be analysed both as a set of images (multispectral reflectography) and as a set of reflectance spectra at different spatial points. The painting layers are partially transparent to NIR wavelengths thus allowing us to tailor in-band imaging to the reflectance contrast response of the various hidden features, e.g. repaintings and preparatory drawings [4]. Moreover, thanks to the variegate reflectance of the painting materials in the Vis-IR range, spectral imaging is effective in the discrimination of pigments [5].

Holistic multispectral imaging can be jointly used with pointwise and scanning analytical techniques to gain more comprehensive information on materials distribution. The multi-technique approach is being widely applied in the field of cultural heritage: joint use of hyperspectral imaging and spectrometry in the Vis-IR is reported in the study of paintings [6] and manuscripts [7]; X-Ray fluorescence (XRF) spectroscopy is complementary to reflectance imaging in the identification of pigments as shown in recent examples on paintings [8-10], manuscripts [7], and in archaeology [11].

The ambitious objective of a full-field and noninvasive mapping of pigments requires careful integration of multimodal spectrometry and imaging techniques and the issue is still an open research field. A common problem concerning the use of hand-held XRF spectrometer is to have at disposal an optimized procedure for the selection of the sampling points and the spatial registration to the spectral images.

Modern instrumentations based on scanning technology allow capturing large and high-quality datasets that can be processed by means of statistical approaches. Principal Component Analysis (PCA) and classification methods as Spectral Angle Mapper (SAM) and Spectral Correlation Mapper (SCM) are used to analyze spectra similarities in multispectral and hyperspectral imaging [12-13,7,10]. Statistical PCA analysis is applied to XRF dataset from scanning techniques or from single-point spectrometers as shown in recent examples on paintings [14], manuscript [15], printed books [16], archaeology [17].

In this work, we demonstrate a workflow based on PCA analysis for integrating multispectral Vis-IR imaging with XRF spectrometry aimed at mapping pigments in large paintings. Firstly, the two datasets coming from XRF pointwise spectrometry and multispectral imaging are fused in a unified representation. Then, PCA is used for analyzing the effectiveness of this representation compared to analyzing the two data-set separately.

The method was applied to support the restoration phase of a “telero”, namely a large canvas painting, by Carpaccio at the Gallerie dell’Accademia museum in Venice. The work was the pilot study for the systematic restoration of the entire Saint Orsola cycle by the artist, on display at the Venetian museum. The characterization of pigments is clearly a mandatory task during the restoration phase of a painting. Even if XRF spectrometry on a discrete set of spots is being performed as a common practice in the museum, apart from simple characterization, no work was still done dealing with statistical analysis aimed at integrating spectral imaging and XRF spectra for analyzing such large canvas.

2. Materials and methods

2.1 The Carpaccio’s “teleri”

Vittore Carpaccio (c. 1460-1526) was one of the major artists in Venice between the end of the XV and the beginning of the XVI century, who also held the role of “official painter” of the Republic of Venice. Among his masterpieces, the cycle of Legend of Saint Orsola, an ensemble of nine large “teleri” representing the legend of Saint Orsola, was the first official commission for the young Carpaccio, entirely executed in the 1490s. Down the centuries, the entire cycle was restored many times in an effort to conserve and to transmit the beauty of the paintings to the future generations. Three restoration interventions were reported in the XVI century, when Carpaccio was still alive, followed by numerous other conservation works between the XVII and the XX century and eventually in 1982-1984 [18]. The last intervention has been recently carried out in 2016-2019. The entire Saint Orsola cycle is on display at the Gallerie dell'Accademia museum in Venice.

The paintings analyzed in this work is the sixth "telero" of the cycle, "The meeting of the pilgrims with the Pope" (279x305cm), probably executed between 1493 and 1495. The data here presented were collected to gather information about the artwork before the restoration campaign.

2.2 Multispectral Vis-IR image dataset

The multispectral image stack includes 16 channels in the Vis range from 380 to 780 nm and 16 channels in the IR from 750 to 2550 nm. Data have been acquired with the multispectral Vis-NIR scanner device of the European infrastructure "Iperion CH" that provides access to its advanced Mobile Laboratory [19]. It is an advanced device based on multiple sensors able to acquire a set of narrow-band images by raster sampling the surface of the painting with a spatial step of 250 μm and a bandwidth of about 20-30 nm in the Vis range and of about 100 nm in the NIR range, building up a registered stack with unitary magnification on an area of $1m^2$ [20-21].

Multispectral imaging in the Vis-NIR was performed on the entire painting, in multiple sessions, for a total scanning area of 279x305 cm.

2.3 X-Ray fluorescence spectrometry dataset

The XRF dataset presented in this work has been collected to support the identification and have a more exhaustive knowledge about the inorganic pigments composing Carpaccio's red colours palette. The motivation for focusing the analysis on the red palette is that Carpaccio was renewed for his vivid and brilliant reds; indeed, red is the most outstanding colour in this canvas painting, as well as in Carpaccio's production in general.

Because of the large dimension of the canvas, the XRF sampling has been limited to a number of 47 selected points. The spots of interest have been chosen using the multispectral IR image dataset and the IR-Vis false colour image, following the usual scheme for creating the false colour composite image (FCC): IR(950nm)-Red-Green [22]. The areas with different red pigments exhibit different colours in FCC due to the differences in the Vis-IR reflectance spectrum; the retouches usually have a lower reflectance in the IR band compared to the surrounding red pigment and appear as dark areas. In this way, it is possible to distinguish the original and the restored or repainted areas, e.g. hidden layering, materials with similar appearance in the visible that have different reflectance Vis-IR spectra [23]. An alternative approach, as shown in our previous study [13] can be to analyse the reflectance spectra in every single pixel for a first discrimination and clustering. However, due to the dimension of the multispectral cube this approach requires a considerable amount of processing power. The different responses of red areas in the false colour images are instead immediate and easier to use for guiding the pointwise XRF campaign.

Fig. 1 reports the map of the analyzed XRF samples registered to the Vis and false colour image. Vis and false colour images of the selected areas are shown in detail as supplementary material of the paper. Red colour is mostly visible on vestments, cloaks and hats of the figures and on the flags. The false colour response suggests the use of four different red pigments by the artist. According to reference literature in the field [23], red ochre (iron oxide red pigment) shows greenish tones in the false colour image, red lead has a yellow response, vermilion appears as a yellow-orangish colour and red lake as bright orange.

Hence, the XRF has been performed in some selected areas representative of the entire painting: on the vestment, the cape, and the hat of the cardinal in the foreground holding the cross, on the garment of the man next to the Pope, on the hose of the standing man on the left holding a stick, on the hat of the cardinal behind the Pope, on Pope's cloak, on the original and on the restored area in the flags.

For the in situ XRF spectrometry, a Thermo Fisher Scientific Niton XL3t GOLDD+ XRF Analyzer was used with a spatial resolution of 3 mm (diameter of the small-spot collimator), Ag anode, maximum voltage of the X-ray tube up to 50 KV, current of the X-ray tube up to 40 mA, and acquisition time 60 s. The measurement was performed in air. The instrument was kept in contact with the painting by the operator.

Fig.1 The canvas by Carpaccio with the map of the XRF points, acquired with the hand-held spectrometer, registered to the imaging scanner dataset. The IR-Vis false colour response is superimposed to the Vis image in the selected areas of investigation, corresponding to the red mixtures (see also supplementary material of the paper). The colours of the area borders are used for identifying the group in the analysis.

2.4 XRF spectrometry and multispectral data fusion

The process of fusing imaging data with pointwise information from the spectrometer is not straightforward. In this study, we implemented a procedure based on open-source software tools (Python, Scikit-learn [24] and rasterio [25]) for a joint analysis of the XRF spectra and the multispectral data registered in the same spatial position.

The dataset is composed of a file with the XRF data and of a raster file exported in .lan format with the multispectral Vis-IR data. The XRF data contains the coordinates and the corresponding counts per element of the selected points. In this study, the spatial position of the spot taken with the hand-held spectrometer has been manually registered to the image cube. This operation was rapid and accurate because the multispectral scanner device produces aberration-free images with unitary magnification; of course, advance scanning XRF instrumentation can be used for automatic multimodal acquisition. The resulting data set is composed of a multispectral cube in which to the selected spots are referenced the corresponding XRF data. At the coordinates of each XRF point we extract the reflectance data from the multispectral image cube. The XRF spectra were pre-processed extracting the maximum counts of most representative peaks of each element detectable by the instrument.

The whole procedure can be summarized as follows:

1. The multispectral scan is performed on the artwork.
2. The XRF set of selected points, guided by the image data and taken with the hand-held spectrometer, are spatially referenced to the multispectral image cube.
3. The Vis-IR reflectance values on each spot where the XRF analysis was performed are extracted (to overcome the issue of the different spatial resolution of the two instruments, the reflectance spectrum is the result of an average of the region of interest (ROI) corresponding to the XRF spot size).
4. The resulting Vis-IR reflectance vector is joined with the corresponding XRF spectrum on the same spot (normalization of the two spectra can be applied before joining the vectors).
5. The PCA is used on the resulting matrix of joint reflectance-XRF for extracting the information.

For validating this procedure, the PCA computed using this workflow is compared against the PCA computed on the two data sets (XRF and reflectance from the multispectral cube) taken individually. The PCA analysis was specifically built for the project using Python and the open-source library Scikit-learn [24]. The plotting of the results was performed using matplotlib [26]. Different approaches for pre-processing heterogeneous data were tested using combination of min-max normalization on the two datasets separately, or directly applying a standardization of the joint data set. In the final approach the data has been standardized subtracting the mean and scaling to unitary variance. After this step we computed the PCA.

Supporting Information for:

Integration of multispectral visible-infrared imaging and pointwise X-ray fluorescence data for the analysis of a large canvas painting by Carpaccio

N de Manincor[a], G Marchioro[b], E Fiorin[c], M Raffaelli[d], O Salvadori[c], C Daffara[b]*

[a] Dept. of Cultures and Civilizations, Viale dell'Università 4, 37129 Verona, Italy
[b] Dept. of Computer Science, University of Verona, Strada le Grazie 15, 37134 Verona, Italy
[c] Gallerie dell'Accademia di Venezia, Scientific Laboratory of Misericordia, Cannaregio 3553, 30121 Venice, Italy
[d] CNR - National Institute of Optics, Largo Enrico Fermi 6, 50125 Florence, Italy

This Digital Supporting Information (DSI) reports additional information not included in the text related to false colour imaging and PCA analysis.

1. False colour imaging

False colour imaging IR (950nm-R-G) built from Vis-IR scanner data is used to guide the selection of the XRF representative spots sampled with the hand-held spectrometer in areas of interest corresponding to the Carpaccio's red pigments.

The following detailed images are reported in support of the results discussed in section **2.3 X-Ray fluorescence spectrometry dataset** and are related to figure 1 of the paper (hereby also reported) that showed the map of the XRF spots registered to the imaging dataset.

Fig.1 of the paper. The canvas by Carpaccio with the map of the XRF points, acquired with the hand-held spectrometer, registered to the imaging scanner dataset. The IR-Vis false colour response is superimposed to the Vis image in the selected areas of investigation, corresponding to the red mixtures.

Fig.DSI-1 Detail of the flags in the background. Vis and Vis-IR false colour with the map of the XRF points.

Above, in the false colour image of the **area of the flags**, we can clearly distinguish dark areas (areas with lower reflectance) of extensive retouching. The bright orange colour in the Vis-IR false colour response suggests the use of **red lake** as original pigment, as later confirmed by XRF analysis (see Table 1 in the paper). Here, **points 1-7,12-13,17-19,21** are representative of restored areas, **points 8-11,14-16,20,32-34** are representative of original areas.

Fig.DSI-2 Detail of Pope Ciriaco and cardinals. Vis and Vis-IR false colour with the map of the XRF points.

The false colour image of the **area with the Pope and cardinals** above immediately shows the use of four red pigments in the vestments, cloaks and hats of the figures: the greenish colour corresponds to **red ochre (points 26,27-28,30-31,38-39,47)**, the yellow-orangish tones refer to **vermilion (points 23-24,29,36-37,40)**, yellow colour is representative of **red lead (points 25,35,46)**, and the bright orange response identifies **red lake (points 41-43).** See also Table 1 in the paper.

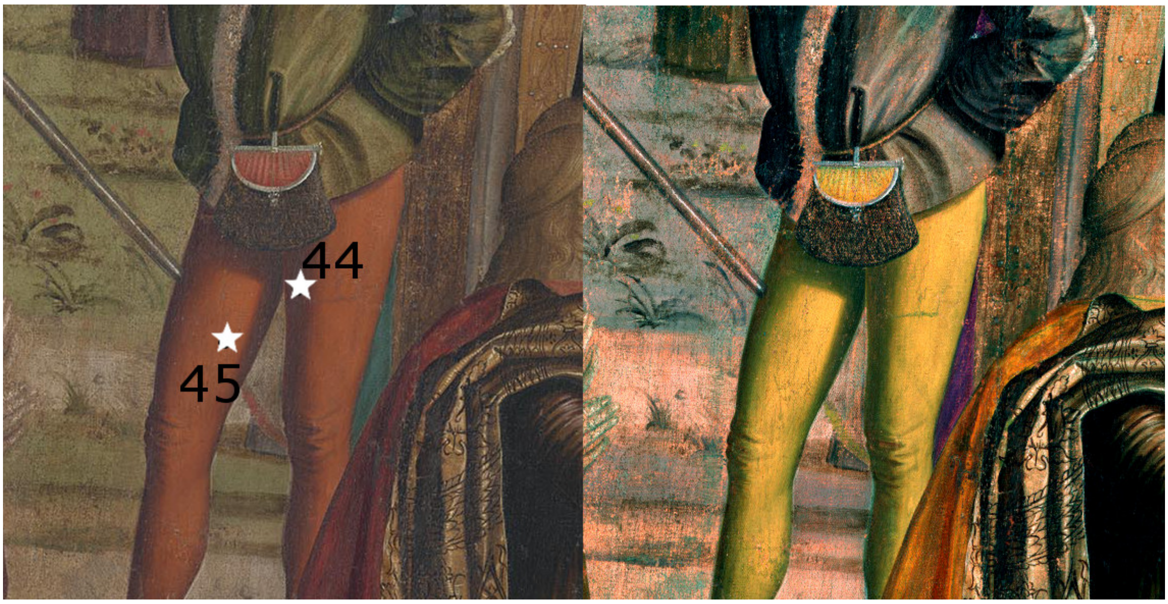

Fig.DSI-3 Detail of scalco's hose. Vis and Vis-IR false colour with the map of the XRF points.

The false colour above suggests the use of **red lead** for the enlighted part and of **red ochre** (probably a superimposed layer) for the shadow. XRF analysis performed in two points, corresponding to the light **(point 45)** and shaded **(point 44)** areas confirmed this suggestion (see Table 1 in the paper).

2. PCA analysis

PCA analysis is used to validate the integrated dataset built fusing the Vis-IR reflectance spectra extracted from the multispectral image cube of scanner with the XRF data sampled in the same spatial position. The PCA on the integrated dataset is compared to the PCA performed on all the single datasets taken individually (Vis reflectance, IR reflectance, as well as Vis-IR reflectance and XRF).

The following plots are reported in support of the results discussed in section **3.2 PCA-based analysis of the integrated dataset** and are related to figure 4 of the paper (hereby also reported) that showed the PCA computed on the fused dataset (Vis-IR+XRF) in comparison to the single XRF and Vis-IR dataset, acquired from the instruments.

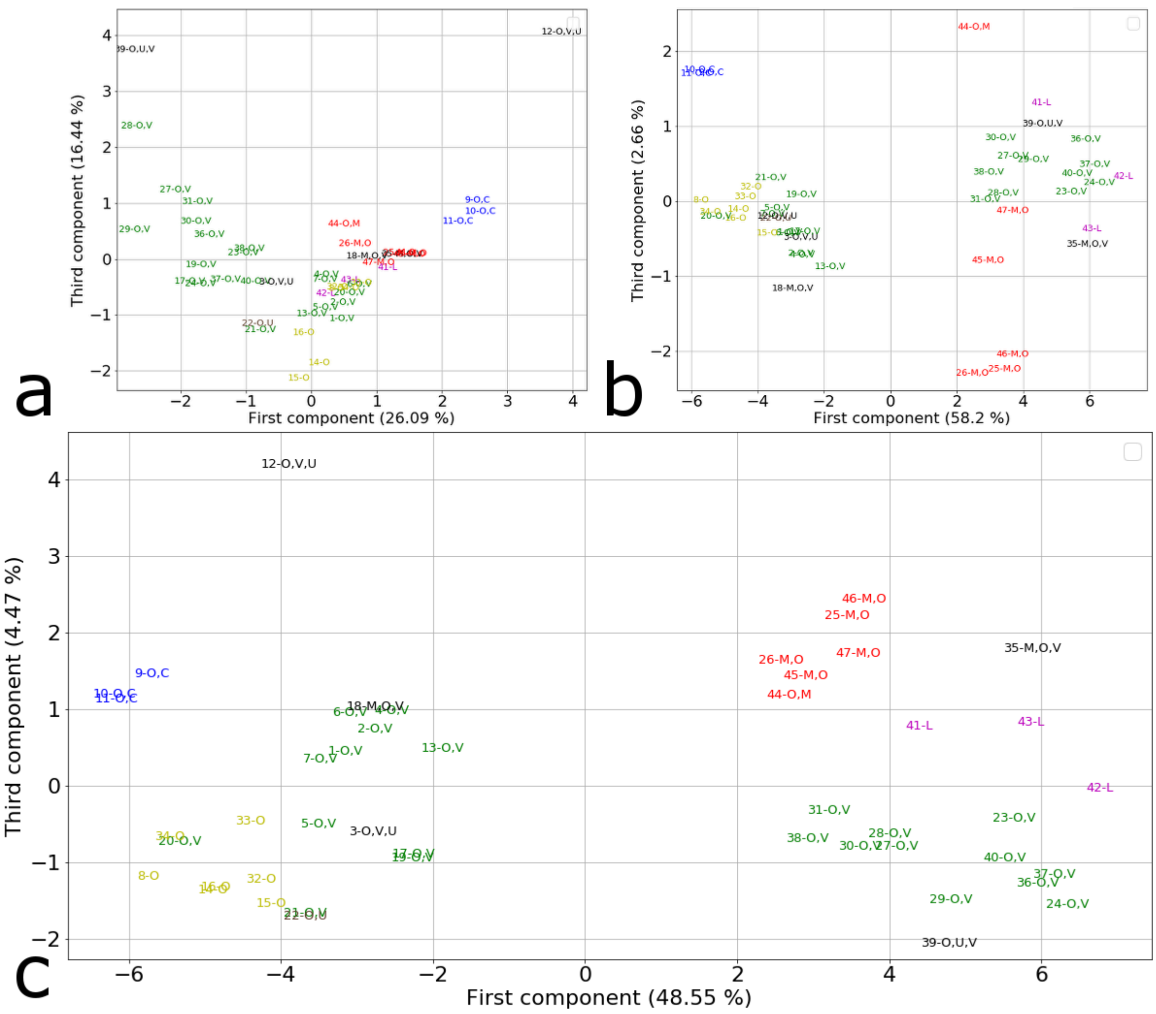

Fig.4 of the paper. The PCA computed on the fused dataset is compared against the PCA computed on the two datasets taken individually in order to validate the integration method: (a) PCA on the **single XRF** dataset, (b) PCA on the **single Vis-IR** reflectance dataset, (c) PCA on the **joint Vis-IR + XRF** dataset.

All the samples with negative scores on the first principal component are part of the area with the flags.

Legend: M: Minium (Red Lead); O: Red Ochre; V: Vermilion; L: Red Lake; C: Copper based pigment; U: Umber. In this case, samples with the same colour have the same composition.

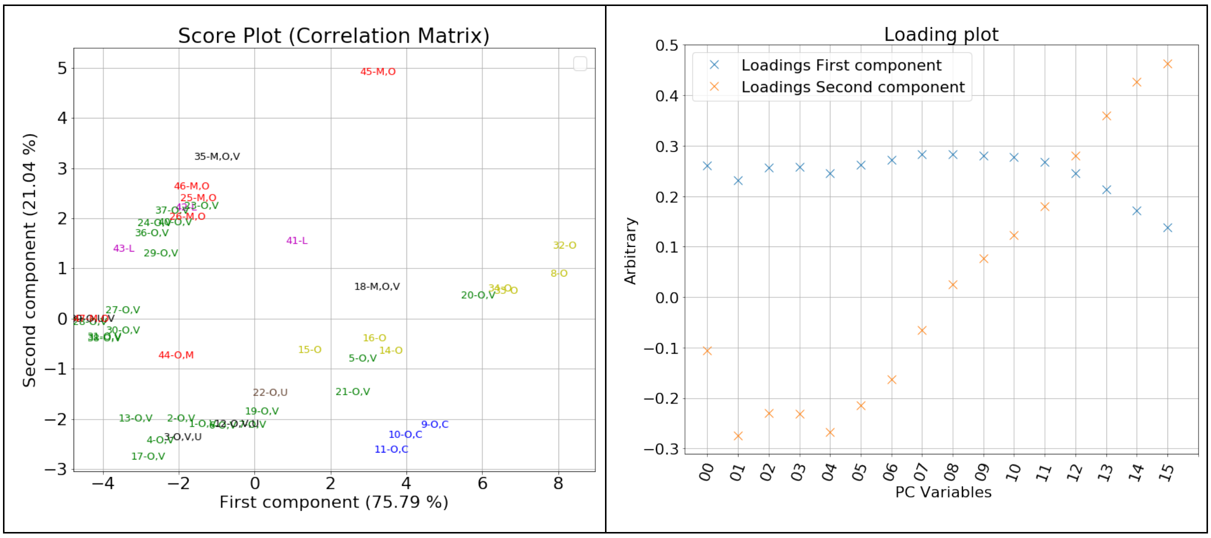

Channels #	00	01	02	03	04	05	06	07	08	09	10	11	12	13	14	15
Wavelenghts (nm)	395	415	455	485	510	530	550	570	590	610	630	650	675	705	735	765

Fig.DSI-4 PCA score plots and loading plots: **single Vis** reflectance scanner dataset.

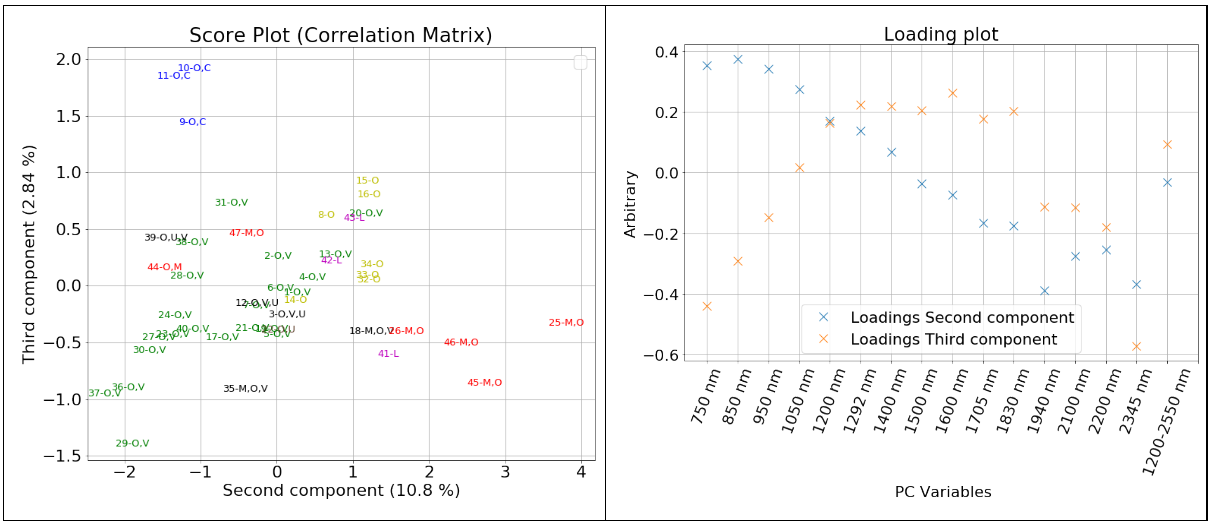

Fig.DSI-5 PCA score plots and loading plots: **single IR** reflectance scanner dataset.

Legend: M: Minium (Red Lead); O: Red Ochre; V: Vermilion; L: Red Lake; C: Copper based pigment; U: Umber. In this case, samples with the same colour have the same composition.

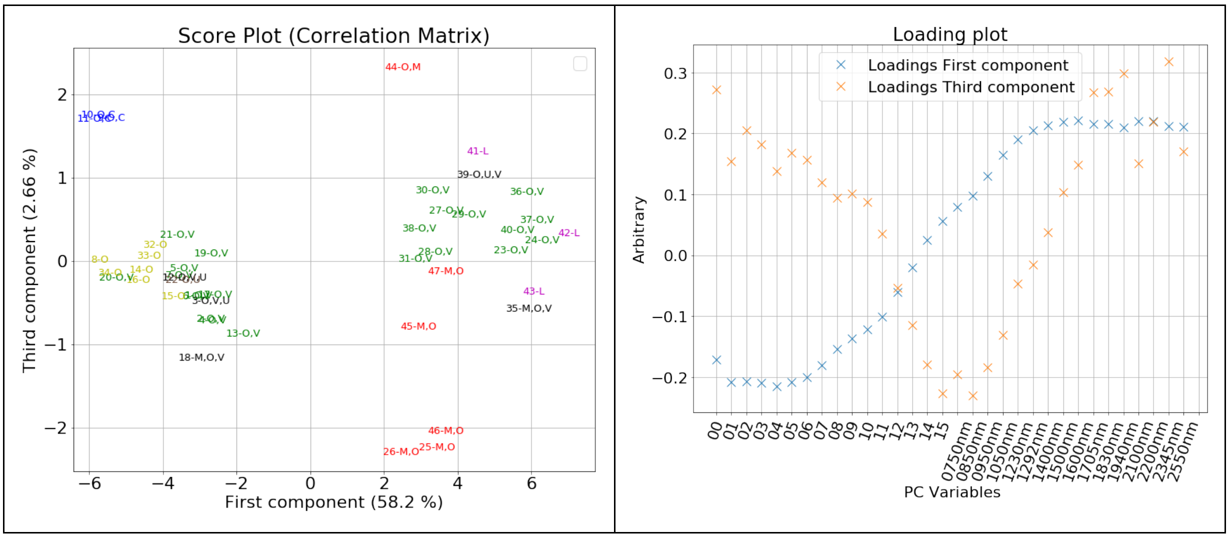

Channels #	00	01	02	03	04	05	06	07	08	09	10	11	12	13	14	15
Wavelenghts (nm)	395	415	455	485	510	530	550	570	590	610	630	650	675	705	735	765

Fig.DSI-6 PCA score plots and loading plots: **single Vis-IR** reflectance scanner dataset.

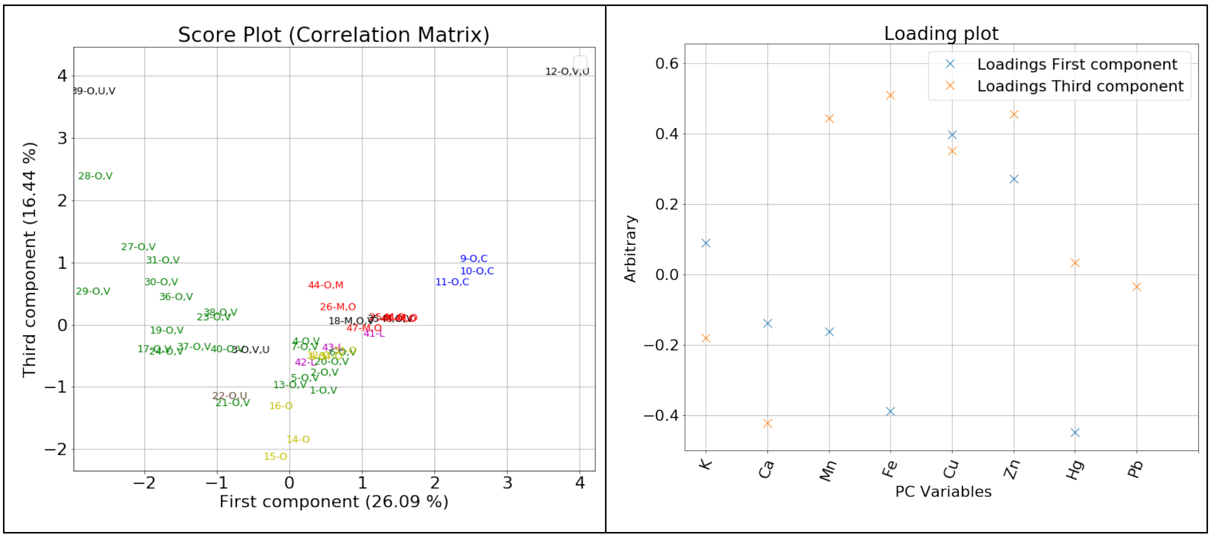

Fig.DSI-7 PCA score plots and loading plots: **single XRF** spectrometer dataset.

Legend: M: Minium (Red Lead); O: Red Ochre; V: Vermilion; L: Red Lake; C: Copper based pigment; U: Umber. In this case, samples with the same colour have the same composition.

3. Results and Discussion

3.1 Elemental XRF analysis

Previous studies on the Carpaccio's artistic technique and stratigraphy [27-29] are helpful for the interpretation of the XRF but need to be corroborated by experimental evidences. From previous studies we can see that the red painted areas were usually obtained with the application of only one or two brushstrokes. In the red palette of Carpaccio's artworks, all the pigments commonly in use in that period are being found: vermilion, red lead, red ochre, red lake and, less extensively, realgar. Vermilion or red ochre were often used as first paint layering, over which red lake was applied as a glaze in the shadows; red ochre was often used, sometimes mixed with earth pigments (umber), for shaded areas; red lead was mostly employed alone.

As mentioned before, the IR-Vis false colour image (reported in Fig. 1 and as supplementary material of the paper), preliminary inspected to guide the XRF sampling, has suggested the use of four red pigments, as well as the presence of a repainted area in the flags in the background.

The elemental results obtained for the different red pigments are summarized in Table 1 and hereby discussed in detail.

In the red mixture of the vestment of the cardinal (**points 27-31**) the discriminating detected elements are Hg and Fe; in the hat (named "biretta") (**points 23-24**) the XRF spectra show high counts of Hg and low counts of Fe. The XRF results and the green colour of IR-Vis false colour image of the garment of the area (Fig. 1) suggest that the artist first spread a thin layer of vermilion, then covered it with a layer of red ochre, especially in the dark shadows of the folds. Even in the hat, vermilion with a modest quantity of red ochre have been employed, but here probably red lake was used as a glaze in the shaded area, as suggested by orangish false colour response.

The same applies to the red mixture of the garment of the standing man next to the Pope (**points 35-40**), greenish in the false colour image, where Hg and Fe have been detected, with higher counts of Hg in relation to Fe in the half-tone area (**points 37,40**) and lower in the shadow area (**points 38,40**). The results suggest that the artist employed vermilion as the first paint layer, then covering it with red ochre in different quantities, whether the area was light or dark. In **point 39**, Mn has also been found, indicating the use of umber in the shadow; while in **point 35**, which corresponds to one of the highlights of the folds on the right, appearing yellow IR-Vis false colour image, Pb counts are higher than Hg and Fe, suggesting that red lead was spread over the layers of vermilion and red ochre. Moreover, from the orangish shades of the false colour response in the half-tones and in the folds shades, we cannot exclude the use of red lake, that cannot be detected by the XRF analysis.

The XRF data acquired on the cape (named "mozzetta") of the cardinal with the cross (**points 25-26**), on the hose of the standing man on the left (**points 44-45**), and on the hat of a cardinal behind the Pope (**points 46-47**) indicate Pb as principal element; Fe is present in all the collected points, with higher counts in the shaded regions (**points 26,44,47**). With reference to the false colour image, we can assume that the artist used the red lead as principal pigment in the enlightened areas (yellow in false colour), superimposing the red ochre for shadows rendering (greenish shades in false colour).

Three spots investigated on Pope's cloak, representative of highlight, half-tone and shadow (**points 41-43**), are characterized by XRF spectra containing Pb and low counts of Fe, and absence of Hg. The orange colour in the IR-Vis false colour image suggests red lake as the principal pigment, with a moderate quantity of red ochre. Higher counts of Pb in **point 41** reveal the use of white lead for obtaining the highlight.

The XRF analysis of the red mixture in the flags original areas (**points 8-11,14-16,20,32-34**) indicates low counts of Fe and no Hg. As in the case of Pope's cloak, the orange false colour suggests the use of a red lake as principal pigment, spread in different thicknesses for obtaining light areas (modulated with white lead) or half-tone and dark areas, and mixed to a moderate quantity of red ochre. In the "pentimento" in the flag on the left (**points 8-11**) the counts of Cu, associated to a copper based green pigment (not possible to distinguish by means of XRF alone), increase, indicating that Carpaccio executed this area on revisiting the work, after having already completed the mountain behind it.

Regarding the red mixtures of the restored parts (**points 1-7,12-13,17-19,21**), the XRF analyses show the constant presence of Hg and Fe, with higher counts of Fe in the shadows and higher counts of Hg in the highlights and half-tones; in the three spots (**points 3,12,22)** of the darker areas, low counts of Mn have also been detected. These results suggest the use of vermilion and red ochre pigments, and in some cases umber in the shadows, during the restoration intervention.

Table1
Identified main elements in the studied samples

Areas and spots	Identified elements by XRF	Identified pigments
Cardinal in the foreground holding the cross, vestment Points 27-31	Ca, Fe, Hg, Pb	Vermilion, Red Ochre
Cardinal in the foreground holding the cross, hat (*biretta*) Points 23-24	K, Ca, Fe, Hg, Pb	Vermilion, Red Ochre, Red Lake (IR-Vis false colour image)
Standing man next to the Pope, garment Points 35-40	K, Ca, Mn, Fe, Hg, Pb	Vermilion, Red Ochre, Umber, Red Lead (IR-Vis false colour image)
Cardinal in the foreground holding the cross, cape (*mozzetta*) Points 25-26	Ca, Fe, Pb	Red Lead, Red Ochre

Scalco, hose Points 44-45	Ca, Fe, Pb	Red Lead, Red Ochre
Cardinal behind the Pope, hat Points 46-47	K, Ca, Fe, Pb	Red Lead, Red Ochre
Pope, cloak Points 41-43	K, Ca, Fe, Pb	Red Lake (IR-Vis false colour image), Red Ochre, White Lead
Flags, original area Points 14-16,20,32-34	K, Ca, Fe, Pb	Red Lake (IR-Vis false colour image), Red Ochre
Flags, *pentimento* Points 8-11	K, Ca, Fe, Cu, Pb	Red Lake (IR-Vis false colour image), Red Ochre, a Copper Based Green Pigment
Flags, restored area Points 1-7,12-13,17-19,21	K, Ca, Mn, Fe, Cu, Zn, Hg, Pb	Vermilion, Red Ochre, Umber

3.2 PCA-based analysis of the integrated dataset

The following discussed results are reported as supplementary material of the paper. In the analysis of the Vis and IR bands information as separated contributions, only the Vis score plot with the first and the second principal component, explaining 96% of the variance, shows two clusters that can be linked with the location of the samples on the canvas. Here we can identify two groups, corresponding one to the area of the flags and the other to the vestments. Instead, the IR score plot with the first and the second principal component doesn't show well defined clusters. The PCA model with the first two principal components on joint Vis-IR data explains 93% of the variance and identifies two clusters, flags and vestments, as well, but no additional information regarding the type of pigments can be extracted. The whole XRF data set can be represented as a 47x8 matrix. However, performing the PCA over XRF data set alone, does not highlight any clear cluster on the score plot as in the case of the IR score plot.

When we performed the PCA with the first two principal components on the joint Vis-IR reflectance and XRF data represented as a 47x40 matrix, with no standardization applied (Fig. 2), the XRF contribution is higher than the multispectral contribution. This is clear in the loading plots (shown as supplementary material), in which both the first and the second principal component of the multispectral data weight almost zero. The score plot representation is hence very similar to the one of the XRF data singularly analysed.

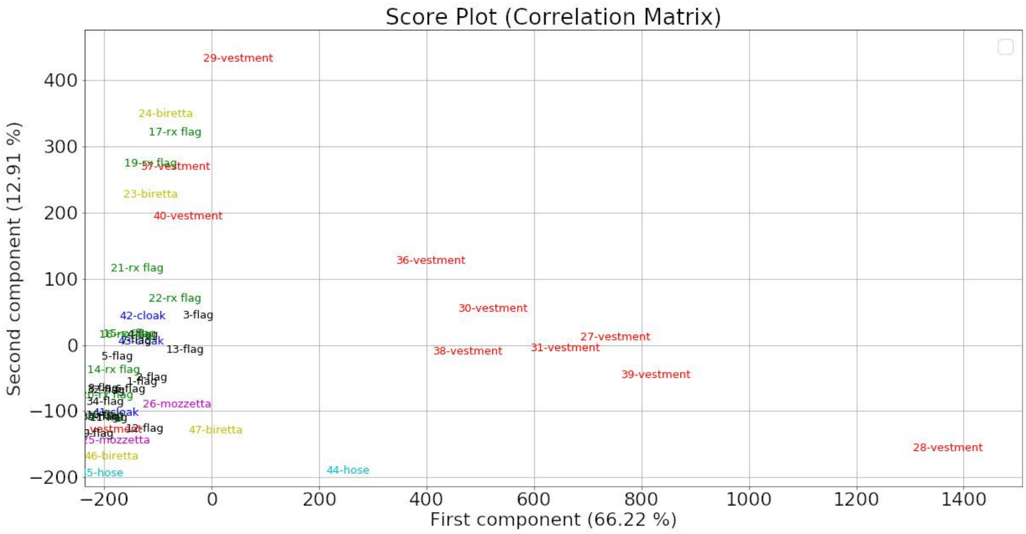

Fig. 2 PCA of the joint Vis-IR and XRF dataset

To optimize our dataset, we decided to normalize all the data to 255, corresponding to the maximum encoded value of the reflectance spectra, and to apply two different scaling methods. With a min-max scaler we have been able to distinguish the big clustering groups of flags and vestments in the PCA model with the first two principal components (Fig. 3). We achieved the best results applying a standardization method, whose plot with the first principal component against the third principal component shows two clusters that can be assigned to the locations (flags or vestments), but also distinguishes different clusters representing the various pigments which are not visible on the elaboration of the separated XRF and reflectance data set. In Fig. 4 the clusters of the vestments with vermilion, red lead, red ochre and red lake predominance are highlighted. In the flags clusters we can group the points in the area of the original “pentimento”, where Cu counts are present, due to the copper based pigment used to paint the mountain in the background, and the points of the restored areas with higher counts of Ca, probably indicating the calcium carbonate of the “stucco”, or the calcium carbonate of the preparatory ground, over which the restoration works were directly performed.

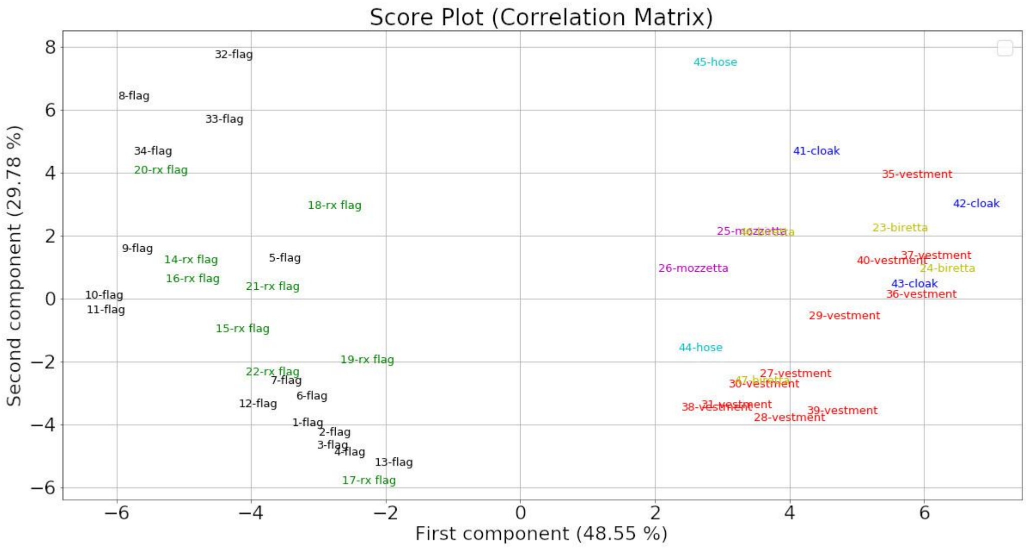

Fig. 3 PCA of the joint Vis-IR and XRF dataset with minmax normalization

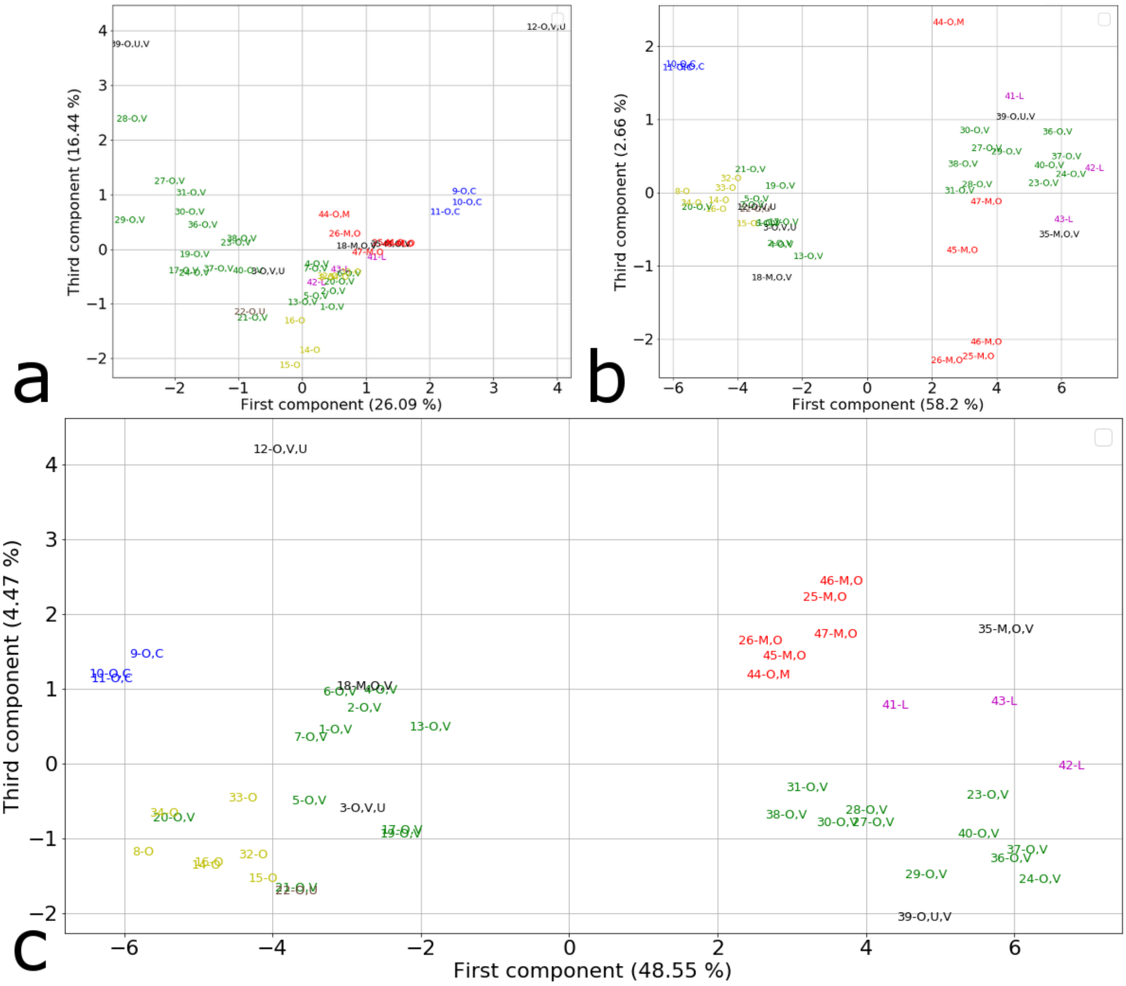

Fig.4 The PCA computed on the fused dataset is compared against the PCA computed on the two datasets taken individually in order to validate the integration method: (a) PCA on the single XRF dataset, (b) PCA on the single Vis-IR reflectance dataset, (c) PCA on the joint Vis-IR and XRF dataset applying the standardization.

Legend: M: Minium (Red Lead); O: Red Ochre; V: Vermilion; L: Red Lake; C: Copper based pigment; U: Umber. In this case, samples with the same colour have the same composition. All the samples with negative scores on the first principal component are part of the area with the flags.

As final discussion to complete the above analysis, as shown in the loading plots (in supplementary materials) we can observe that most of the channels contributes to the clustering. Hence, we can state that the distinction is not based on a single feature but rather on the sum of contributions from various spectral bands. Furthermore, we have to consider that the variance explained from each component is not only linked with the signal of the red pigments but also with the influences of the other components of the pictorial layers. This is clear from the fact that we distinguish two clusters: one related to the measurements carried out in the compromised area of the flag.

4. Conclusion

A data fusion methodology for integrating multispectral reflectance data in the Vis-IR with single spot XRF information was presented. The PCA has been employed to investigate the potentialities of the fused dataset. The PCA-based integrated methodology is demonstrated on the red painted areas of “The meeting of the pilgrims with the Pope”, a large canvas by Carpaccio, which has been investigated before the last restoration intervention (2016-2019).

Using this method, we were able to identify well defined clusters linked to the different red pigments used by the artist and to the conservation history of the painting. These clusters were not detectable when analysing the dataset independently.

When PCA is performed on the Vis-IR reflectance data of the scanner we can distinguish two main clusters, corresponding to the vestments area and to the area of the flag. On the joint data we tested different methods to normalize our heterogeneous dataset. The standardization has been proved the most effective because we clearly distinguish the location clustering and the pigments identification clustering. The approach can be later extended for fusing data coming from other imaging and pointwise techniques in an automated and replicable way once the analyses have been properly registered.

Acknowledgements

This work was partially supported by the Scan4Reco project funded by the European Union Horizon 2020 Framework Programme for Research and Innovation under grant agreement no 665091.

References

[1] H. Liang, Advances in multispectral and hyperspectral imaging for archaeology and art conservation, Appl. Phys. A-Mater. 106 (2012) 309–323. https://doi.org/10.1007/s00339-011-6689-1.

[2] K. Janssens, G. Van der Snickt, F. Vanmeert, S. Legrand, G. Nuyts, M. Alfeld, L. Monico, W. Anaf, W. De Nolf, M. Vermeulen, Non-invasive and non-destructive examination of artistic pigments, paints, and paintings by means of X-ray methods, Top. Curr. Chem. 374 (2016) 81. https://doi.org/10.1007/s41061-016-0079-2.

[3] M. Alfeld, L. de Viguerie, Recent developments in spectroscopic imaging techniques for historical paintings-a review, Spectrochim. Acta B. 136 (2017) 81–105. https://doi.org/10.1016/j.sab.2017.08.003.

[4] C. Daffara, R. Fontana, Multispectral infrared reflectography to differentiate features in paintings, Microsc. Microanal. 17 (2011), 691-5. https://doi.org/10.1017/S1431927611000031.

[5] C. Cucci, J.K. Delaney, M. Picollo, Reflectance hyperspectral imaging for investigation of works of art: old master paintings and illuminated manuscripts, Acc. Chem. Res. 49 (2016) 2070–2079. https://doi.org/10.1021/acs.accounts.6b00048.

[6] J.K. Delaney, J.G. Zeibel, M. Thoury, R. Littleton, M. Palmer, K.M. Morales, E.R. de La Rie, A. Hoenigswald, Visible and infrared imaging spectroscopy of Picasso’s Harlequin musician:

mapping and identification of artist materials in situ, Appl. Spectrosc. 64 (2010) 584–594. https://doi.org/10.1366/000370210791414443.

[7] C. Cucci, S. Bracci, A. Casini, S. Innocenti, M. Picollo, L. Stefani, I.G. Rao, M. Scudieri, The illuminated manuscript corale 43 and its attribution to Beato Angelico: non-invasive analysis by FORS, XRF and hyperspectral imaging techniques, Microchem. J. 138 (2018) 45–57. https://doi.org/10.1016/j.microc.2017.12.021.

[8] J.K. Delaney, K.A. Dooley, R. Radpour, I. Kakoulli, Macroscale multimodal imaging reveals ancient painting production technology and the vogue in Greco-Roman Egypt, Sci. Rep. 7 (2017) 15509. https://doi.org/10.1038/s41598-017-15743-5.

[9] K.A. Dooley, D.M. Conover, L.D. Glinsman, J.K. Delaney, Complementary standoff chemical imaging to map and identify artist materials in an early Italian Renaissance panel painting, Angew. Chem. Int. Ed. 53 (2014) 13775–13779. https://doi.org/10.1002/anie.201407893.

[10] J. Striova, C. Ruberto, M. Barucci, J. Blažek, D. Kunzelman, A. Dal Fovo, E. Pampaloni, R. Fontana, Spectral imaging and archival data in analysing Madonna of the Rabbit paintings by Manet and Titian, Angew. Chem. Int. Ed. 57 (2018) 7408–7412. https://doi.org/10.1002/anie.201800624.

[11] M. Alfeld, M. Mulliez, J. Devogelaere, L. De Viguerie, P. Jockey, P. Walter, MA-XRF and hyperspectral reflectance imaging for visualizing traces of antique polychromy on the Frieze of the Siphnian Treasury, Microchem. J. 141 (2018) 395–403. https://doi.org/10.1016/j.microc.2018.05.050.

[12] H. Deborah, S. George, J.Y. Hardeberg, Pigment Mapping of the Scream (1893) Based on Hyperspectral Imaging, in: A. Elmoataz, O. Lezoray, F. Nouboud, D. Mammass (Eds.), Image and Signal Processing. ICISP 2014. Lecture Notes in Computer Science, vol 8509, Springer, Cham, 2014, pp. 247–256. https://doi.org/10.1007/978-3-319-07998-1_28.

[13] N. de Manincor, G. Marchioro, V. Barra, O. Salvadori, C. Daffara, Optical characterization of artist's materials in ancient paintings by spectral imaging in the VIS-IR range, in: J. Beyerer, F. Puente Leon, T. Langle (Eds.), OCM 2017 - Optical Characterization of Materials - Conference Proceedings, KIT Scientific Publishing, 2017, pp. 137–148. https://doi.org/10.5445/KSP/1000063696.

[14] F. Rosi, A. Burnstock, K.J. Van den Berg, C. Miliani, B.G. Brunetti, A. Sgamellotti, A non-invasive XRF study supported by multivariate statistical analysis and reflectance FTIR to assess the composition of modern painting materials, Spectrochim. Acta B. 71 (2009) 1655–1662. https://doi.org/10.1016/j.saa.2008.06.011.

[15] S. Legrand, P. Ricciardi, L. Nodari, K. Janssens, Non-invasive analysis of a 15th century illuminated manuscript fragment: point-based vs imaging spectroscopy, Microchem. J. 138 (2018) 162–172. https://doi.org/10.1016/j.microc.2018.01.001.

[16] F. Albertin, E. Balliana, G. Pizzol, G. Colavizza, E. Zendri, D. Raines, Printing materials and technologies in the 15th–17th century book production: An undervalued research field, Microchem J. 138 (2018) 147–153. https://doi.org/10.1016/j.microc.2017.12.010.

[17] I. Marcaida, M. Maguregui, H. Morillas, N. Prieto-Taboada, S.F.-O. de Vallejuelo, M. Veneranda, J.M. Madariaga, A. Martellone, B. De Nigris, M. Osanna, In situ non-invasive

characterization of the composition of Pompeian pigments preserved in their original bowls, Microchem. J. 139 (2018) 458–466. https://doi.org/10.1016/j.microc.2018.03.028.

[18] F. Valcanover, Le storie di Sant'Orsola di Vittore Carpaccio dopo il recente restauro, Atti Dell'Istituto Veneto di Scienze, Lettere ed Arti (1986) 196–209

[19] IPERION CH Integrated Platform for the European Research Infrastructure ON Cultural Heritage, Molab facility. http://www.iperionch.eu/molab/ (accessed 6 September 2019).

[20] C. Bonifazzi, P. Carcagni, R. Fontana, M. Greco, M. Mastroianni, M. Materazzi, E. Pampaloni, L. Pezzati, D. Bencini, A scanning device for VIS–NIR multispectral imaging of paintings, J Opt. A-Pure Appl. Op. 10 (2008) 064011. https://doi.org/10.1088/1464-4258/10/6/064011.

[21] R. Fontana, M. Barucci, E. Pampaloni, J. Striova, L. Pezzati, From Leonardo to Raffaello: insights by Vis-IR reflectography, in: D. Hradil, J. Hradilová (Eds.), Acta Artis Academica 2014 - Interpretation of Fine Art's Analysis in Diverse Contexts, Academy of Fine Arts in Prague, 2014, pp. 15–26.

[22] A. Aldrovandi, D. Bertani, M. Cetica, M. Matteini, A. Moles, P. Poggi, P. Tiano, Multispectral Image Processing of Paintings, Stud. Conserv. 33(3) (1988) 154–159. https://doi.org/10.2307/1506208.

[23] T. Moon, M.R Schilling, S. Thirkettle, A note on the use of false-colour infrared photography in conservation, Stud. Conserv. 37(1) (1992) 42–52. https://doi.org/10.2307/1506436.

[24] F. Pedregosa, G. Varoquaux, A. Gramfort, V. Michel, B. Thirion, O. Grisel, M. Blondel, P. Prettenhofer, R. Weiss, V. Dubourg, Scikit-learn: Machine learning in Python, J. Mach. Learn. Res. 12 (2011) 2825–2830.

[25] S. Gillies et al. , Rasterio: geospatial raster I/O for Python programmers, https://github.com/mapbox/rasterio, 2013.

[26] J.D. Hunter, Matplotlib: A 2D graphics environment, Comput. Sci. Eng. 9 (2007) 90–95. https://doi.org/10.1109/MCSE.2007.55.

[27] L. Lazzarini, Il colore nei pittori veneziani tra il 1480 e il 1580, Bollettino d'Arte (supplement 5) (1983) 135–144.

[28] G.N. Sciré, S. Rossi (Eds.), Vittore Carpaccio: tre capolavori restaurati, Marsilio, Venezia, 2007.

[29] D. Radeglia (Ed), L'arrivo a Colonia di Vittore Carpaccio: Studio e restauro, Gangemi Editore, 2015.